JOURNAL OF Materials CHEMISTRY

Design, synthesis and photophysical properties of C_{60}-modified proteins

Hiroto Murakami,[a] Rika Matsumoto,[b] Yuko Okusa,[b] Takamasa Sagara,[b] Mamoru Fujitsuka,[c] Osamu Ito*[c] and Naotoshi Nakashima*[b]

[a]*Institute for Fundamental Research of Organic Chemistry, Kyushu University, Hakozaki, Fukuoka, 812-8581, Japan*
[b]*Department of Materials Science, Graduate School of Science and Technology, Nagasaki University, Bunkyo, Nagasaki, 852-8521, Japan. E-mail: nakasima@net.nagasaki-u.ac.jp*
[c]*Institute of Multidisciplinary Research for Advanced Materials, Building of Chemical Reaction Science, Tohoku University, Katahira, Sendai, 980-8577, Japan*

Received 31st January 2002, Accepted 22nd February 2002
First published as an Advance Article on the web 28th March 2002

Fullerene–porphyrin conjugates coordinated with Fe and Zn ions (**1**·Fe and **1**·Zn) were designed and synthesized. Compounds **1**·Fe and **1**·Zn were reconstituted into apomyoglobin successfully to produce C_{60}-modified myoglobins, **1**·Fe-Mb and **1**·Zn-Mb, respectively. The axial-ligand exchange reaction revealed that **1**·Fe-Mb maintains the intrinsic properties of native Mb, except for the autooxidation rate constant, suggesting similar microenvironment of the porphyrin moieties in the proteins. Cyclic voltammogram (CV) of a graphite electrode modified with a film of **1**·Fe-Mb–didodecyldimethylammonium bromide (DDAB) showed two reversible redox couples with $E^{0\prime} = -206$ and -1048 mV which are attributable to $Fe^{2+/3+}$ and the reduction of the porphyrin ring, respectively. Differential pulse voltammogram of an electrode modified with a **1**·Fe-Mb–tridodecylmethylammonium bromide (TDAB) film in water containing 0.5 M tetraethylammonium chloride and 10 mM 2,2′,2″-nitrilotriethanol showed three cathodic peaks at $E_{1/2,1} = -372$, $E_{1/2,2} = -555$, and $E_{1/2,3} = -1028$ mV which are attributable to $Fe^{2+/3+}$, $C_{60}{}^{0/1-}$, and the reduction of the porphyrin ring, respectively. The electrodes modified with **1**·Fe-Mb and **1**·Zn-Mb gave anodic photocurrent coupled with on–off light irradiation. The action spectrum of photocurrent for a **1**·Zn-Mb–DDAB film was in accord with the UV–vis absorption spectrum of **1**·Zn-Mb. Transient absorption spectra of **1**·Zn in benzonitrile and **1**·Zn-Mb in a 50 mM phosphate buffer at 100 ns after the ns-laser light pulse irradiation at 532 nm showed three absorption maxima at 700, 830, and 1000 nm which are assignable to the triplet excited state of C_{60} ($^3C_{60}$*), the triplet excited state of the zinc porphyrin (^{3}ZnP*), and C_{60} radical anion ($C_{60}{}^{\bullet-}$), respectively. Existence of the apparent $C_{60}{}^{\bullet-}$ indicates the generation of charge-separation state, $ZnP^{\bullet+}$–$C_{60}{}^{\bullet-}$. The rate constants for the generation of the charge separation states in **1**·Zn and **1**·Zn-Mb calculated from the fluorescence data were 8.2×10^8 s^{-1} and 6.4×10^8 s^{-1}, respectively, and the corresponding quantum yields were 0.62 and 0.59.

Introduction

Water soluble fullerene derivatives possess biological activities including antiviral activity against HIV,[1,2] selective DNA cleavage,[2] and promotion of chondrogenesis.[3] However, because of their high hydrophobic nature, fullerenes themselves are insoluble in aqueous solution, and hence application of fullerenes to the biological field has been rather limited. To overcome this problem, the following strategies have been attempted: the complexation with cyclodextrin,[4] solubilization of fullerenes in liposomes[5] and in poly(vinylpyrrolidone)[6] aqueous solution, and introduction of hydrophilic groups[7] to fullerenes. Introduction of a fullerene moiety into water-soluble biomolecules is also such a strategy that can create novel fullerene-biomaterials with specific functions.[8] Our objective is to design and synthesize a water-soluble fullerene–protein conjugate and to characterize it to develop a novel function. Success in the construction of biodevices based on fullerene–protein conjugated novel materials would promise potential biological, biochemical, pharmaceutical and medical applications. Son and coworkers reported a fullerene-modified protein in which methano[C_{60}]fullerene dicarboxylic acid was covalently attached to the amino-residues of native and denatured bovine serum albumin.[9] Hill and coworkers described the preparation and electrochemical behavior of a fullerene-modified redox protein, azurin mutant S118C, prepared by site-directed mutagenesis methods followed by chemical modification.[10]

Our strategy for preparing a fullerene-modified protein is to use the heme protein reconstitution method.[11] By substitution of hemin of proteins with hemin derivatives, reconstituted artificial proteins can be prepared. We have recently reported the preparation and characterization of reconstituted C_{60}-modified myoglobin (**1**·Fe-Mb), in which the prosthetic group consists of fullerene–porphyrin conjugate (**1**·Fe).[12] This modified protein would be of interest as the functional component of artificial photosynthetic systems since fullerenes raise the efficiency of photoinduced charge separation.[13] We describe herein in detail the design, synthesis, and photophysical properties of reconstituted myoglobins modified with C_{60} (**1**·Fe-Mb and **1**·Zn-Mb), in which the center metal of the prosthetic group is iron or zinc, respectively (Chart 1).

Results and discussion

Design and synthesis of fullerene–porphyrin conjugates

To suppress the structural perturbation in the reconstituted Mb, a hexamethylene spacer was introduced between the fullerene moiety and protoporphyrin.[14] Fullerene–protoporphyrin conjugates, **1**·Fe and **1**·Zn, were synthesized according to

 DOI: 10.1039/b201145j

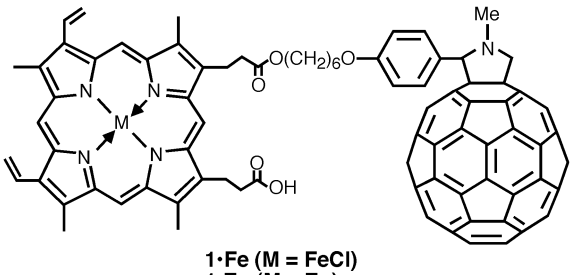

1·Fe (M = FeCl)
1·Zn (M = Zn)

Chart 1

Scheme 1. The reaction of C_{60} with *N*-methylglycine and 4-(6-hydroxyhexyloxy)benzaldehyde (**2**) in chlorobenzene produced 1′-methyl-2′-[4-(6-hydroxyhexyloxy)phenyl]-2′,3′,4′,5-tetrahydropyrrolo[3′,4′:1,2][60]fullerene (**3**), which was condensed with protoporphyrin (acid chloride form) in the mixed solvent of CH_2Cl_2–CS_2 = 2 : 3 (v/v) to give a fullerene–porphyrin conjugate **1**. Iron or zinc insertion into **1** in dry DMF produced **1**·Fe and **1**·Zn, respectively. All compounds obtained were identified by ^{1}H NMR, IR, UV–vis, MS spectroscopies, and elemental analysis. Regioisomers were not separated in this study.

Optimized structure of fullerene–porphyrin conjugates

The molecular orbital calculations with PM3-level[15] were performed to elucidate the optimized structure of **1**·Zn. Two conformations were obtained with similar heat of formations; one is the extended structure and another is the bent structure as shown in Fig. 1a and b, respectively. In the bent structure, there may be an interaction between the fullerene moiety and the Zn-porphyrin (ZnP) moiety. On the other hand, the extended structure may be favorable for reconstitution to apomyoglobin.

Reconstitution of fullerene–porphyrin conjugates to apomyoglobin

Reconstitution of **1**·Fe and **1**·Zn with apomyoglobin (apo-Mb) was conducted by slight modification to standard procedure.[16–18] From UV–vis spectral measurements, the concentrations[19] of the obtained **1**·Fe-Mb and **1**·Zn-Mb solutions were determined to be 3.9 and 3.7 μM, respectively.

Aqueous buffer solution (pH 7.5) of **1**·Fe-Mb and **1**·Zn-Mb showed positive circular dichroism (CD) bands at 408 and 420 nm, respectively. Induction of CD arises from the incorporation of **1**·Fe or **1**·Zn into the heme crevice of apo-Mb.

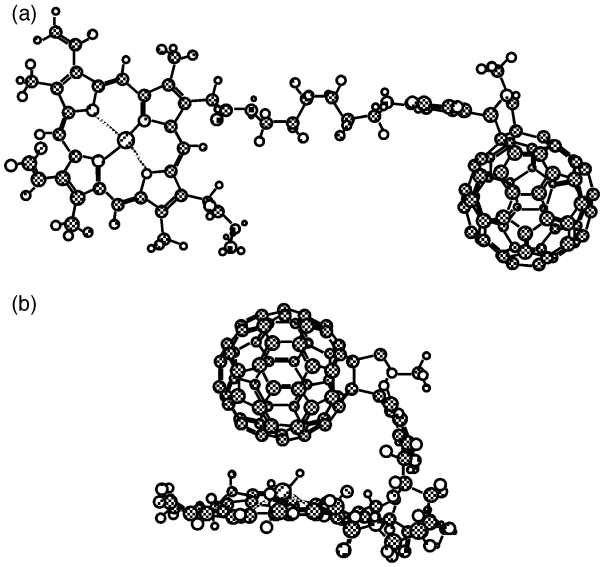

Fig. 1 Optimized structures of **1**·Zn obtained by PM3 calculation; (a) extended structure and (b) bent structure.

The C_{60}-protein **1**·Fe-Mb was characterized by axial-ligand exchange reaction with H_2O to fluoride or azide ion and reduction–oxygenation reaction. Fig. 2 shows UV–vis absorption spectra of **1**·Fe-Mb alone and in the presence of sodium azide or potassium fluoride. The absorption maxima of the Soret- and Q-bands of **1**·Fe-Mb (met-form) appeared at 408 nm and 504 and 630 nm, respectively, which are very close to those of native Mb (met-form, Soret-band: 408 nm, Q-bands: 502 and 630 nm, respectively).[20] The Soret- and Q-bands of **1**·Fe-Mb in the presence of sodium azide appeared at 419 nm and 538 and 571 nm, respectively, which are also close to those of corresponding native Mb (Soret-band: 418 nm, Q-bands: 540 and 572 nm)[20] in the presence of azide ion. The Soret- and Q-bands of **1**·Fe-Mb in the presence of potassium fluoride were 407 and 602 nm, which are close to those of corresponding native Mb (Soret-band: 406 nm, Q-bands: 604 nm)[20] in the presence of potassium fluoride.

As shown in Fig. 2, the addition of sodium dithionate to the buffer solution of **1**·Fe-Mb (met-form) produced **1**·Fe^{II}-Mb,

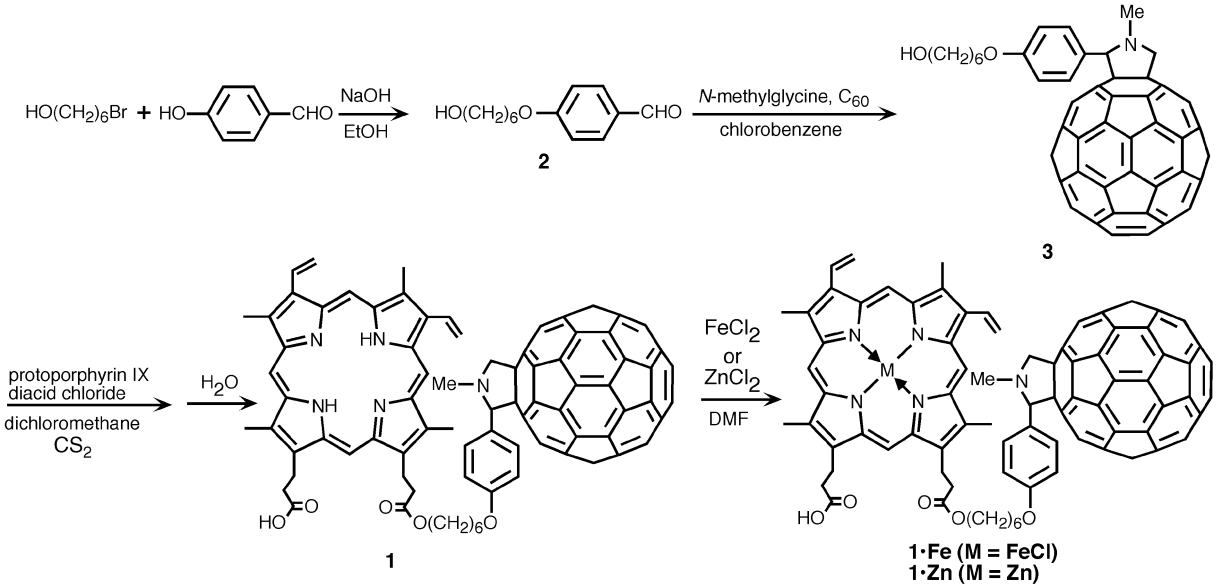

1·Fe (M = FeCl)
1·Zn (M = Zn)

Scheme 1

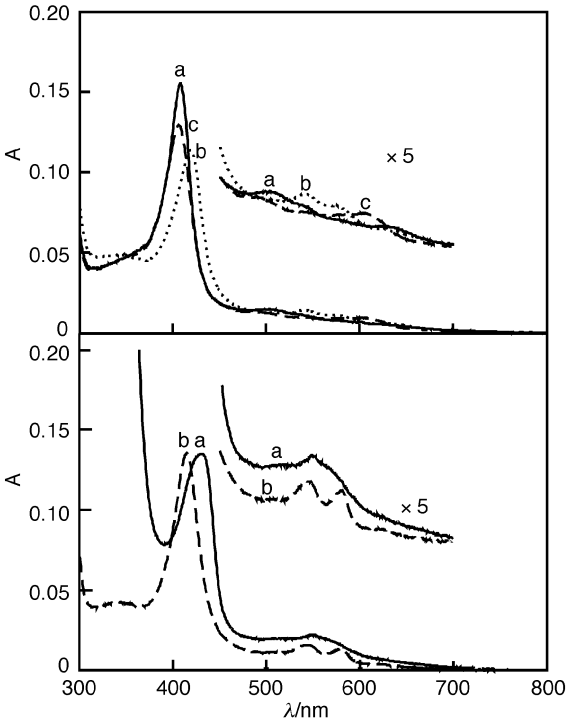

Fig. 2 Above: UV–vis absorption spectra of (a) **1**·Fe-Mb alone and (b) in the presence of NaN_3 or (c) KF in a 50 mM phosphate buffer (pH 7.5). Below: UV–vis absorption spectra of (a) **1**·Fe-Mb in a 50 mM phosphate buffer after the addition of aliquots of $Na_2S_2O_4$, (b) followed by dioxygen bubbling.

showing Soret- and Q-bands at 431 and 557 nm, respectively, which are close to those of corresponding native Mb(Fe^{II}) (Soret-band: 435 nm, Q-band: 556 nm). When dioxygen was introduced, the reduced **1**·Fe^{II}-Mb was found to form the oxygen complex whose Soret- and Q-bands appeared at 415 nm and 543 and 578 nm, respectively, which are very close to those of the oxygen complex of native Mb (Soret-band: 418 nm, Q-bands: 541 and 578 nm).[20] The stability of the oxygen complex of **1**·Fe-Mb was monitored by the time course of the absorbance of the Q-band at 578 nm. The oxy-form of **1**·Fe^{II}-Mb was gradually autooxidized to the met-form with the first-order rate constant of 0.2 h^{-1}, which is *ca.* 6-times larger than that of native Mb measured under the same experimental conditions. The observed faster autooxidation could be due to the introduction of the bulky fullerene moiety to the protein. These results suggest that the heme moieties in **1**·Fe-Mb and native Mb are located in similar microenvironments. A schematic representation of **1**·Fe^{II}-Mb is presented in Fig. 3.

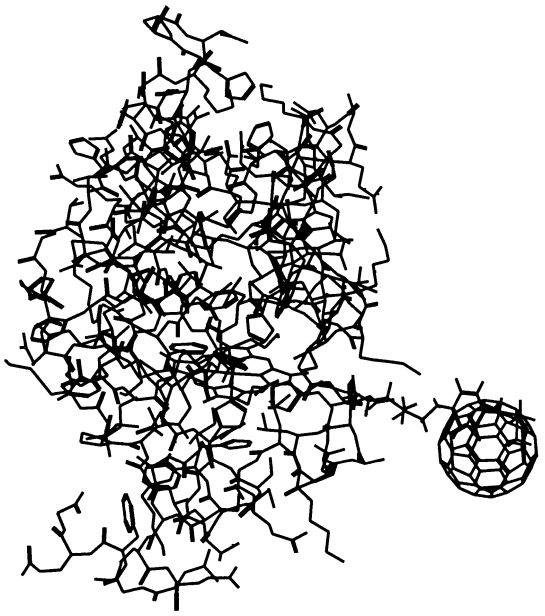

Fig. 3 A schematic representation for **1**·Fe-Mb.

Cyclic voltammetry

Lipid cast films on electrodes have been reported to provide suitable microenvironments for the electron transfer of Mb.[21] We employed didodecyldimethylammonium bromide (DDAB) as a lipid.

Fig. 4a shows a typical cyclic voltammogram of a BPG electrode modified with a **1**·Fe-Mb–DDAB film in a 50 mM phosphate buffer (pH 7.5). Two redox couples were observed at $E^{o\prime} = -206$ and -1048 mV which are attributable to $Fe^{2+/3+}$ and the reduction of the porphyrin ring, respectively.[22] CV for a pyrolytic graphite electrode (BPG) modified with a native Mb–DDAB film in a 50 mM phosphate buffer (pH 7.5) showed two redox couples at $E^{o\prime} = -318$ and -1048 mV (data are not shown). The observed 112 mV positive shift in the CV for the metal in **1**·Fe-Mb compared with that of native Mb suggests that the microenvironments around the metals are different. Peak separations of the redox couples for the metal and the ring in **1**·Fe-Mb at 100 mV s^{-1} were 27 and 35 mV, respectively, which are smaller than 58 mV, suggesting that the redox current at the electrode is from the surface-confined species of **1**·Fe-Mb in the film.

The peak current of the redox couple for the metal in **1**·Fe-Mb was proportional to the scan rate in the range from 20 to 200 mV s^{-1} (Fig. 4b), as expected for thin-layer electrochemical behavior. Peak separations of the redox couples for the metal and the ring in native Mb at 100 mV s^{-1} were 65 and 35 mV, respectively. Rusling and coauthors reported that native Mb–DDAB-modified BPG showed diffusion-kinetic-controlled

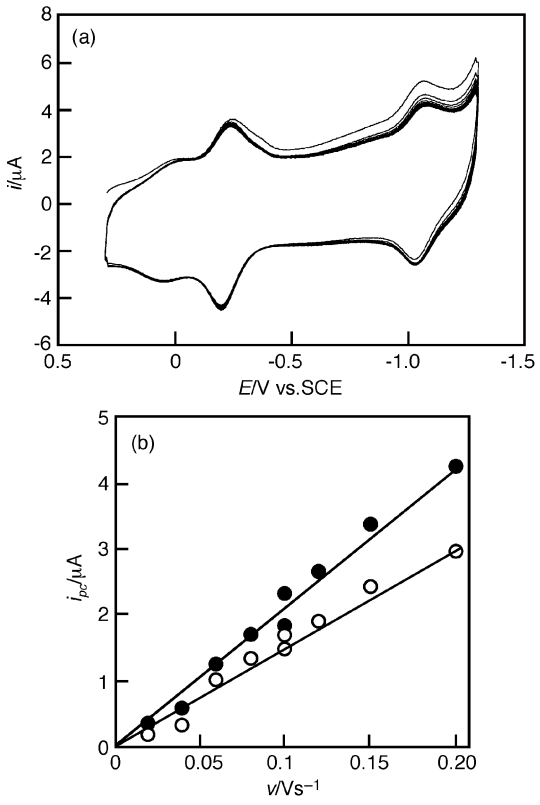

Fig. 4 (a) CV for a fully loaded **1**·Fe-Mb–DDAB film on a BPG electrode in a 50 mM phosphate buffer (pH 7.5). Scan rate to cathodic direction, 100 mV s^{-1}. (b) Scan rate dependence of i_{pc} (open circle) and i_{pa}(closed circle) for the redox couple of $Fe^{3+/2+}$ in the **1**·Fe-Mb–DDAB film.

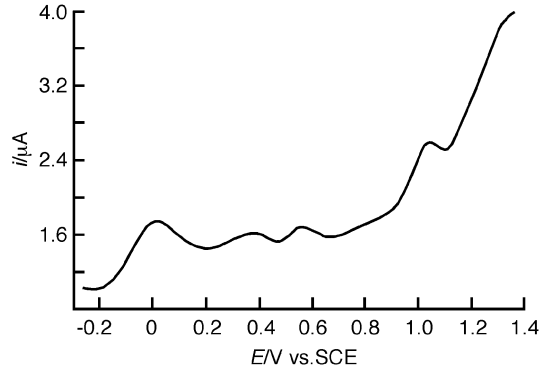

Fig. 5 DPV for a fully loaded **1**·Fe-Mb–TDAB film on a BPG electrode in water containing 0.5 M TEAC. Scan rate = 20 mV s^{-1}; pulse amplitude = 20 mV.

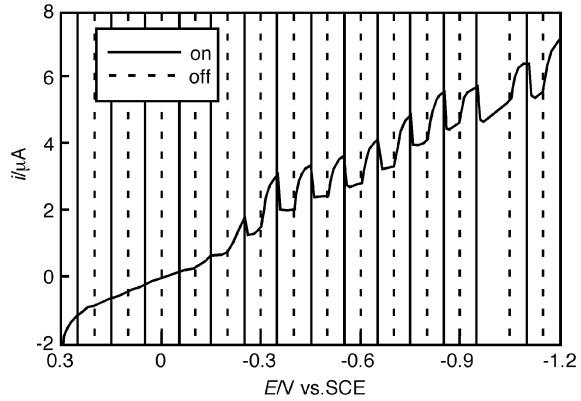

Fig. 6 Current change coupled with on–off UV light irradiation *vs.* potential for a fully loaded **1**·Fe-Mb–DDAB film on a BPG electrode in a 50 mM phosphate buffer (pH 7.5) containing 10 mM TEOA and 10 mM KBr. Scan rate = 1 mV s^{-1}. UV light on–off irradiation was carried out alternately at every 50 s interval.

electrochemical behavior at the scan rates above 50 mV s^{-1} and thin-layer electrochemical behavior at the scan rates below 6 mV s^{-1}.[22] The difference in the electrochemical behavior may be caused by a structural change of two different composite films. An electrode modified with the **1**·Zn-Mb–DDAB film gave no redox couples in the CV in the potential range from 0.3 to −1.2 V. This result is not unusual because zinc Mb is electroinactive in this potential range in water.

We could not see a redox couple for the C_{60} moiety of **1**·Fe-Mb (see Fig. 4a). The following two reasons are considered for this behavior: i) the redox current of the fullerene moiety hides behind the current of $Fe^{3+/2+}$ of Mb and ii) the C_{60} moiety of the **1**·Fe-Mb–DDAB film on the electrode is electroinactive. The electrochemical properties of fullerenes are known to be influenced by electrolyte and matrix.[23] Hence, we used tetraethylammonium chloride (TEAC) as an electrolyte and tridodecylmethylammonium bromide (TDAB) instead of DDAB as a matrix lipid, and then measured a differential pulse voltammogram (DPV) of a **1**·Fe-Mb–DDAB modified electrode. As shown in Fig. 5, we see three cathodic peaks at $E_{1/2,1} = -372$, $E_{1/2,2} = -555$, and $E_{1/2,3} = -1028$ V, which are attributable to $Fe^{2+/3+}$, $C_{60}^{0/1-}$, and the reduction of the porphyrin ring, respectively.[24,25] The peak which appears at −8 mV in Fig. 5, as well as the CV response around 0 mV in Fig. 4a, are the background peaks from the BPG electrode surface.

Photoelectrochemical measurement

Photoelectrochemical measurements were conducted for fully loaded **1**·Fe-Mb–DDAB films and **1**·Zn-Mb–DDAB films on BPG electrodes in a 50 mM phosphate buffer (pH 7.5) containing 10 mM triethanolamine† (TEOA) and 10 mM KBr. Typical current response coupled with on–off UV light irradiation for the **1**·Fe-Mb electrode is shown in Fig. 6. Anodic photocurrent was observed at the potential below −0.2 V, which is close to the redox potential of $Fe^{2+/3+}$ in **1**·Fe-Mb. Maximal photocurrent obtained was 1.56 μA at −0.85 V. The electrode modified with a **1**·Zn-Mb–DDAB film also gave anodic photocurrent. The photocurrent of **1**·ZnMb was 17 nA at −0.8 V, that is, 100-fold smaller than that at the **1**·Fe-Mb electrode. This difference may come from the nature of the metal coordinated to the porphyrins. Under the same experimental conditions, photocurrent was not observed for native Mb–DDAB and zinc Mb–DDAB film-modified electrodes. These data indicate that the fullerene moieties in **1**·Fe-Mb and **1**·Zn-Mb contribute to generation of the observed photocurrent.

We also examined wavelength dependence of the photocurrent. As can be seen in Fig. 7, the action spectrum of a

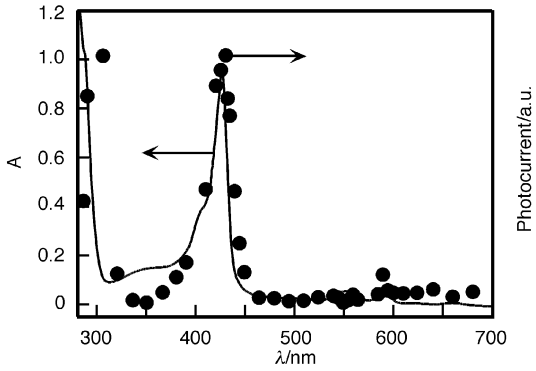

Fig. 7 Photocurrent action spectra at −900 mV *vs.* SCE for a **1**·Zn-Mb–DDAB (closed circle) and the UV–vis absorption spectrum (solid line) of **1**·Zn-Mb in a 50 mM phosphate buffer containing 10 mM TOAE and 10 mM KBr.

1·Zn-Mb–DDAB film is in good agreement with the UV–vis absorption spectrum of **1**·Zn-Mb in a 50 mM phosphate buffer. Fig. 7 indicates that in the wavelength range longer than 380 nm, the origin of the photocurrent is photo-excitation of ZnP moiety in **1**·Zn-Mb. These data suggest that the photo-induced charge-transfer from the excited sate of the porphyrin moiety to the fullerene moieties in **1**·Fe-Mb and **1**·Zn-Mb takes place to generate the photocurrent.

Fluorescence lifetime measurements

Fullerene-linked zinc porphyrins are well known as a model of the charge-separation (CS) process in photosynthesis.[26] The CS process of fullerene-linked porphyrins, except for the study[27] using self-assembled monolayers on electrodes, has been carried out in organic solvent because of the lack of solubility of fullerene moiety in water. Hence, we examined CS behavior of **1**·Zn in benzonitrile and that of **1**·Zn-Mb in water.

Fluorescence lifetime measurements were conducted to determine the rate constants for the charge separation (k_{CS}) and quantum yield (Φ_{CS}) for **1**·Zn in benzonitrile and **1**·Zn-Mb in water. Both fluorescences near 650 nm arising from the ZnP moieties in **1**·Zn and **1**·Zn-Mb decayed biexponentially.[28,29] The lifetimes were calculated to be 0.76 and 2.08 ns for **1**·Zn and 0.88 and 2.53 ns for **1**·Zn-Mb. On employing the lifetimes of ZnP (2.10 ns in benzonitrile) and Zn-Mb (2.10 ns in water) as standard, the rate constants (k_{CS}) for **1**·Zn and **1**·Zn-Mb calculated from the fast components in the fluorescence data were 8.2×10^8 s^{-1} and 6.4×10^8 s^{-1}, respectively, and the corresponding quantum yields (Φ_{CS}) were 0.62 and 0.56, respectively (Table 1). The rate constants for **1**·Zn and

†The IUPAC name for triethanolamine is 2,2′,2″-nitrilotriethanol.

Table 1 Fluorescence lifetimes (τ_f), rate constants (k_{CS}), and quantum yields (Φ_{CS}) for the charge separation processes of **1**·Zn and **1**·Zn-Mb

Compounds	Media	Fluorescence lifetime/ns[a]		k_{CS}/s^{-1}[b]	Φ_{CS}[b]
ZnP	Benzonitrile	2.10 (100%)			
1·Zn	Benzonitrile	0.76 (46%)	2.08 (54%)	8.2×10^8	0.62
Zn-Mb	Phosphate buffer	1.01 (29%)	2.60 (71%)		
1·Zn-Mb	Phosphate buffer	0.88 (46%)	2.58 (54%)	6.4×10^8	0.56

[a]Fluorescence lifetimes of zinc porphyrin (ZnP) moiety were measured at 650 nm. [b]The k_{CS} and Φ_{CS} were evaluated from the following equations;[28,29] $k_{CS} = (\tau_f)^{-1} - (\tau_{f0})^{-1}$ and $\Phi_{CS} = [(\tau_f)^{-1} - (\tau_{f0})^{-1}]/(\tau_f)^{-1}$, where τ_f is the lifetime of **1**·Zn or **1**·Zn-Mb evaluated from the fast component of the two-component decay; τ_{f0} is the lifetime of ZnP or Zn-Mb, in which τ_{f0} of Zn-Mb was evaluated from the average of the two-component decay (2.10 ns).

1·Zn-Mb were about one order of magnitude smaller than that for the fullerene-ZnP dyad linked with rigid amide bonds, in which k_{CS} has been reported to be 9.5×10^9 s^{-1} in benzonitrile.[29] The smaller k_{CS} could be due to the flexible spacer in **1**·Zn. In the charge-separation process from the excited singlet state of zinc porphyrin moiety, the k_{CS} and Φ_{CS} values were not significantly different to those in **1**·Zn and a **1**·Zn-Mb, indicating that the charge-separation process is not sensitive to the structures, bent or stretch structures, and/or to the environments, in benzonitrile or in water.[29]

Laser flash photolysis

We first tried to measure the picosecond transient spectra to confirm the CS process observed by the fluorescence lifetime measurement; however, transient absorption bands assignable to the radical-ion pair were not clearly observed, because of its low concentration. The absorption bands of the radical-ion pair were hidden by the huge transient absorptions of the singlet absorptions ($S_1 \rightarrow S_n$) of the zinc porphyrin moiety in the visible-region and C_{60} moiety in the near-IR region.[29] Thus, we employed the nanosecond laser flash photolysis (laser light pulse = *ca.* 10 ns). The transient absorption spectra of **1**·Zn in benzonitrile are shown in Fig. 8. The spectrum at 100 ns after the laser-light pulse irradiation at 532 nm showed three absorption maxima at 700, 830, and 1000 nm which are assignable to the triplet excited state of C_{60} ($^3C_{60}$*), the triplet excited state of the zinc porphyrin (^{3}ZnP*), and C_{60} radical anion ($C_{60}^{\bullet -}$), respectively.[29] Existence of apparent $C_{60}^{\bullet -}$ indicates the generation of charge-separation state ($ZnP^{\bullet +}$–$C_{60}^{\bullet -}$) in **1**·Zn. The lifetime of $C_{60}^{\bullet -}$ determined by time profile of the absorption at 1000 nm (Fig. 8, inset) was 440 ns, which is comparable to that of a fullerene-ZnP dyad linked with rigid spacer such as amide bonds (580 ns).[28,29]

Transient absorption spectra of **1**·Zn-Mb in a 50 mM phosphate buffer (pH 7.5) at 100 ns after the laser-light pulse irradiation also showed three absorption maxima at 700, 830, and 1000 nm, assignable to $^3C_{60}$*, ^{3}ZnP*, and $C_{60}^{\bullet -}$, respectively (Fig. 9). Remarkably, the lifetime of $C_{60}^{\bullet -}$ for **1**·Zn-Mb (*ca.* 8 μs) was unusually longer than that of **1**·Zn in benzonitrile, while the amount of $C_{60}^{\bullet -}$ generated by the same laser power was poor (Fig. 9, inset). This behavior may come from the structure of **1**·Zn-Mb where ZnP is surrounded by protein.

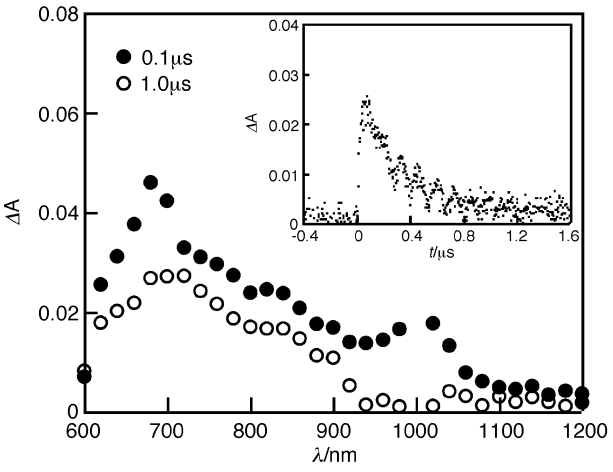

Fig. 8 Transient absorption spectra obtained with 532 nm laser photolysis of **1**·Zn in deaerated benzonitrile at 0.1 μs (closed circle) and 1 μs (open circle). Inset: absorption-time profile at 1000 nm.

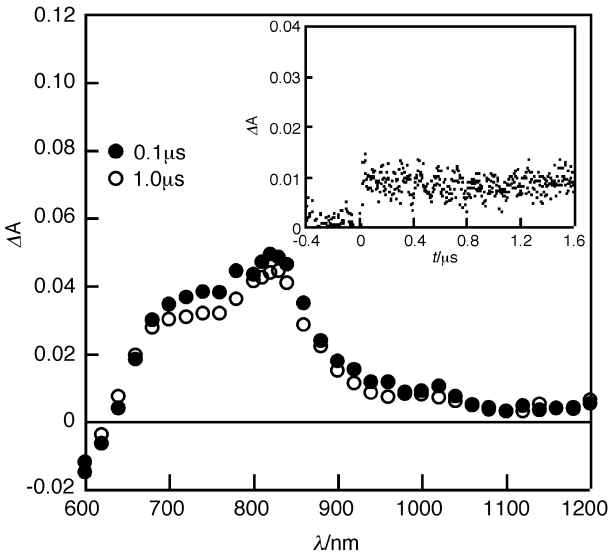

Fig. 9 Transient absorption spectra obtained by 532 nm laser photolysis of **1**-Zn-Mb in deaerated 50 mM phosphate buffer (pH 7.5) at 0.1 μs (closed circle) and 1 μs (open circle). Inset: absorption-time profile at 1000 nm.

In benzonitrile, a charge-recombination process will proceed in the bent form of **1**·Zn, in which fast charge-recombination is expected because of the close proximity of the radical anion of C_{60} and radical cation of ZnP-moieties. In the case of **1**·Zn-Mb, on the other hand, the C_{60}- and ZnP-moieties are expected to have an extended structure due to the steric hindrance of Mb, and the rate for the charge-recombination process will become slower.

Although the fate of the radical ion-pair produced in *ca.* 10 ns was not followed by picosecond transient spectra, the time-profile at 1000 nm of **1**·Zn in benzonitrile may show the mono-exponential decay immediately after the *ca.* 10 ns laser light pulse. On the other hand, most of the radical ion-pair produced in *ca.* 10 ns in **1**·Zn-Mb may decay within the laser pulse and the remaining radical ion-pair may live for a long time up to *ca.* 10 μs.[30]

Conclusions

We designed and synthesized fullerene-porphyrin conjugates, **1**·Fe and **1**·Zn that were successfully reconstituted into apomyoglobin to produce C_{60}-modified myoglobins, **1**·Fe-Mb and **1**·Zn-Mb, respectively. The porphyrin moieties in **1**·Fe-Mb and native Mb were found to be located in similar

microenvironments in the proteins. An artificial Mb, **1**·Fe-Mb could be embedded in a cast film of a lipid and the direct electron transfer reaction of the embedded protein and the underlying electrode was possible. The electrodes modified with **1**·Fe-Mb and **1**·ZnMb gave anodic photocurrent coupled with on–off light irradiation. Laser-light pulse irradiation for the C_{60}-modified myoglobin **1**·Zn-Mb generated $^3C_{60}$*, ^{3}ZnP*, and $C_{60}^{\bullet -}$ whose properties were characterized in detail by nanosecond time-resolved absorption spectroscopy and picosecond time-resolved fluorescence spectroscopy. Photoinduced charge separation takes place *via* the excited singlet state of the porphyrin moiety, producing the radical ion-pair between $C_{60}^{\bullet -}$ and the radical cation of the porphyrin moiety. The radical ion-pair exists in C_{60}-modified myoglobins longer than **1**·Zn in polar solvent.

The present study opens possibilities for the construction of biodevices based on fullerene–protein conjugated novel materials, which promote biochemical, pharmaceutical and medical applications.

Experimental

Materials

Protoporphyrin IX, myoglobin (form horse heart), and C_{60} were obtained from Aldrich, Sigma, and Southern Chemical Group, respectively. Chlorobenzene was distilled once before use. Carbon disulfide and dichloromethane were distilled over $CaCl_2$ and CaH_2 before use, respectively. *N*, *N*-Dimethylformamide was distilled over CaH_2 under reduced pressure before use. Other chemicals and solvents used for synthesis were of reagent grade. Didodecyldimethylammonium bromide was synthesized according to the literature.[31] Tridodecylmethylammonium bromide was obtained *via* ion-exchange of tridodecylmethylammonium chloride (Aldrich). Water was purified through a Milli-Q Puls Ultrapure water system (Millipore); its resistivity was over 18 MΩ cm. Solvents used for spectral and photophysical measurements were of spectral grade. Silica gel 60 (Merck) and Fujisilicia BW 300 were used for thin-layer chromatography and flash-column chromatography, respectively.

Synthesis

4-(6-Hydroxyhexyloxy)benzaldehyde (2). To a solution of 4-hydroxybenzaldehyde (1.5 g, 12 mmol) and 85% sodium hydroxide (0.6 g, 11 mmol) in 50 mL of EtOH, 6-bromohexan-1-ol (2.3 mL, 17 mmol) was added dropwise at room temperature and then the mixture was refluxed for 48 h. After cooling at room temperature, the precipitate was separated and then the filtrate was evaporated. The residue was dissolved in 100 mL of $CHCl_3$ and washed ten times with a 50 mL portion of water, followed by drying over anhydrous $MgSO_4$. The solvent was removed under reduced pressure and then the residue was purified by flash column chromatography on silica gel with $CHCl_3$ as an eluent; yield, 44%. ^{1}H NMR (300 MHz, $CDCl_3$, TMS, 25 °C): δ = 9.9 (s, 1H, CHO), 7.8 (d, 2H, Ar), 6.9 (d, 2H, Ar), 4.0 (t, 2H, CH_2OAr), 3.6 (t, 2H, CH_2OH), 3.4 (t, 1H, OH), 1.4–1.8 (m, 8H, $(CH_2)_4$); IR (neat): ν = 3416 (OH), 1696 (C=O) cm^{-1}. Elemental analysis (%): found (calcd for $C_{13}H_{18}O_3 + 0.5H_2O$): C, 67.32 (67.51); H, 8.08 (8.28).

1′-Methyl-2′-[4-(6-hydroxyhexyloxy)phenyl]-2′,3′,4′,5′-tetrahydropyrrolo[3′,4′:1,2][60]fullerene (3). A solution of C_{60} (1.0 g, 1.4 mmol), *N*-methylglycine (0.34 g, 3.8 mmol), and **2** (0.27 mg, 1.2 mmol) in 400 mL of chlorobenzene was refluxed for 18 h under a N_2 atmosphere and then the solvent was evaporated. Flash column chromatography on silica gel with toluene then $CHCl_3$ as the eluents gave **3** as a brownish black solid; yield, 47%. Mp > 500 °C. ^{1}H NMR (300 MHz, $CDCl_3$, TMS, 25 °C): δ = 7.6, 6.9 (d each, 2H each, ArH), 5.0 (d, 1H, C*H*HN), 4.9 (s, 1H, ArCHN), 4.0 (d, 1H, CH*H*N), 3.7 (t, 2H, CH_2OH), 3.4 (t, 1H, OH), 2.8 (s, 3H, CH_3), 1.2–1.8 (m, 8H, $(CH_2)_4$); IR (KBr): ν = 2931, 2853 (ν_{CH}) cm^{-1}. Elemental analysis (%): found (calcd for $C_{75}H_{23}O_2N + 2.6H_2O$): C, 88.59 (88.59); H, 3.37 (2.80); N, 1.23 (1.38).

2,7,12,18-Tetramethyl-3,8-divinyl-17-(2-carboxyethyl)-13-(2-{6-[4-(1′-methyl-2′,3′,4′,5′-tetrahydropyrrolo[3′,4′:1,2][60]fulleren-2′-yl)phenoxy]hexyloxycarbonyl}ethyl)porphyrin (1). A solution of protoporphyrin IX (180 mg, 0.32 mmol) and oxalyl chloride (3.0 mL, excess amount) in 6 mL of dry CH_2Cl_2 was refluxed for 1 h and then the solvent was evaporated. The acid chloride was obtained as a dark green solid and was dried under reduced pressure and was used for the following reaction without further purification. To a solution of the acid chloride and 4-dimethylaminopyridine (68 mg, 0.56 mmol) in 10 mL of dry CH_2Cl_2, **3** (315 mg, 0.32 mmol) in 15 ml of dry CS_2 was added under a N_2 atmosphere. The reaction mixture was stirred at 45 °C overnight and then the solvents were evaporated. The residue was dissolved in CH_2Cl_2 and washed with alkaline water (pH 8). The organic layer was dried over anhydrous Na_2SO_4 and then the solvent was evaporated. The residue was washed with MeOH followed by $CHCl_3$ and purified by thin-layer chromatography on silica gel with a mixed eluent ($CHCl_3$–MeOH = 20 : 1 v/v) to produced **1** as a purplish black solid; yield, 2.5%. Mp > 500 °C. ^{1}H NMR (400 MHz, $CDCl_3$–CD_3OD = 10 : 1 (v/v), TMS, 25 °C): δ = 10.05–10.20 (m, 4H, *meso*-H), 8.26 (m, 2H, CH=), 7.72, 7.55, 6.54 (d each, J = 7.33 Hz each, 2H each, ArH), 6.19, 6.36 (d each, J = 11.0 Hz, J = 16.9 Hz, 2H each, $=CH_2$), 4.40 (m, 6H, 13^1, 17^1-CH_2, $ArOCH_2$), 4.35 (s, 1H, NCH(Ar)C_{60}), 3.98 (t, 2H, $COOCH_2$), 3.85, 4.72 (d each, J = 9.3 Hz each, 1H each, NCH_2C_{60}), 3.58–3.74 (m, 12H, 2,7,12,18-CH_3), 3.25 (t, 4H, 13^2, 17^2-CH_2), 2.55 (s, 3H, NCH_3), 1.12–1.84 (m, 8H, $(CH_2)_4$); IR (KBr): ν = 2921 (ν_{CH}), 1728 (C=O, ester), 1710 (C=O, carboxylic acid) cm^{-1}; MS: 1517.66 (M^+). Elemental analysis (%): found (calcd for $C_{109}H_{55}O_5N_5 + 8H_2O$): C, 78.57 (78.93); H, 4.42 (4.31); N, 4.62 (4.22). The absorption maxima of Soret- and Q-bands of **1** in $CHCl_3$–MeOH = 10 : 1 (v/v) appeared at 407 nm and 506, 541, 576, and 689 nm, respectively.

[2,7,12,18-Tetramethyl-3,8-divinyl-17-(2-carboxyethyl)-13-(2-{6-[4-(1′-methyl-2′,3′,4′,5′-tetrahydropyrrolo[3′,4′:1,2][60]fulleren-2′-yl)phenoxy]hexyloxycarbonyl}ethyl)porphyrinato]iron(III) chloride (1·Fe). Iron(II) chloride tetrahydrate (17 mg, 130 μmol) was dried under reduced pressure to obtain anhydrous iron(II) chloride. The anhydrous iron(II) chloride and **1** (20 mg, 13 μmol) were dissolved in 5 mL of dry DMF. After stirring for 24 h at 65 °C under a N_2 atmosphere, the solvent was evaporated and then the residue was purified by thin-layer chromatography on silica gel with a mixed eluent ($CHCl_3$–MeOH = 20 : 1 v/v). The obtained solid was washed with 1 mM HCl aqueous solution to obtain **1**·Fe as a black solid. Yield, 13%. Mp > 500 °C. IR (KBr): ν = 3400 (OH), 1730 (C=O, ester), 1710 (C=O, carboxylic acid) cm^{-1}. The absorption maxima of Soret- and Q-bands of **1**·Fe in $CHCl_3$–MeOH = 10 : 1 (v/v) appeared at 403 nm and 489 and 589 nm, respectively.

[2,7,12,18-Tetramethyl-3,8-divinyl-17-(2-carboxyethyl)-13-(2-{6-[4-(1′-methyl-2′,3′,4′,5′-tetrahydropyrrolo[3′,4′:1,2][60]fulleren-2′-yl)phenoxy]hexyloxycarbonyl}ethyl)porphyrinato]zinc(II) (1·Zn). Zinc chloride (27 mg, 200 μmol) and **1** (35 mg, 23 μmol) were suspended in 5 mL of dry DMF and stirred at 65 °C for 12 day under a N_2 atmosphere. The solvent was removed under reduced pressure and then the residue was washed with distilled water to remove an excess amount of zinc chloride. The solid obtained was dried at 50 °C under reduced pressure to give **1**·Zn as a brownish

black solid; yield, 87%. ^{1}H NMR (400 MHz, $CDCl_3$–CD_3OD = 10 : 1 (v/v), TMS, 25 °C): δ = 10.05–10.30 (m, 4H, *meso*-H), 8.38 (m, 2H, CH=), 7.72, 7.57, 6.60 (m each, 2H each, ArH), 6.14, 6.37 (m each, 2H each, $=CH_2$), 4.42 (m, 6H, 13^1, 17^1-CH_2, $ArOCH_2$), 4.29 (s, 1H, $NCH(Ar)C_{60}$), 3.98 (m, 2H, $COOCH_2$), 3.85, 4.72 (m each, 1H each, NCH_2C_{60}), 2.90–3.30 (m, 12H, 2,7,12,18-CH_3), 3.25 (m, 4H, 13^2,17^2-CH_2), 2.64 (s, 3H, NCH_3), 1.12–1.84 (m, 8H, $(CH_2)_4$); IR (KBr): ν = 2921 (ν_{CH}), 1728 (C=O, ester), 1710 (C=O, carboxylic acid) cm^{-1}; MS: 1578.77 (M^+). The absorption maxima of Soret- and Q-bands of **1**·Zn in $CHCl_3$–MeOH = 15 : 2 (v/v) appeared at 418 nm and 546 and 584 nm, respectively.

Preparation of 1·Fe-Mb

The apomyoglobin (apo-Mb) was prepared from horse heart myoglobin by Teale's acid–butanone method.[15] Reconstitution of **1**·Fe and of **1**·Zn with apo-Mb was conducted according to a modified procedure of Yonetani *et al*.[17]

A pyridine solution (100 μL) of **1**·Fe (0.5 mg, 3.3×10^{-7} mol) was added dropwise to an apo-Mb (1.3 mL, 3.3×10^{-7} mol) aqueous phosphate buffer solution (10 mM, pH 7.0) at 4 °C. 20 μL of the buffer solution was added each for one-drop addition of the pyridine solution to maintain the total pyridine content at 10 vol% in the buffer. The precipitate produced was separated by centrifugation (6000 *g*) at 4 °C and then the clear supernatant was purified with Sephadex G-25 equilibrated with a 10 mM phosphate buffer at pH 7.5 to produce **1**·Fe-Mb, which was determined spectrophotometrically.

The preparation of **1**·Zn-Mb was performed in the same manner as that of **1**·Fe-Mb.

Preparation of 1·Fe-Mb (or 1·Zn-Mb)–lipid modified electrodes and electrochemical measurements

The preparation of electrodes modified with **1**·Fe-Mb (or **1**·Zn-Mb) and didodecyldimethylammonium bromide (DDAB) is as follows. 10 μL portions of 0.1 M DDAB in $CHCl_3$ were placed on a basal plane pyrolytic graphite (BPG) electrode (geometric area, 0.25 cm^2) and then allowed to air dry. The lipid-modified electrode was immersed in **1**·Fe-Mb (or **1**·Zn-Mb) solution for 5 days at 4 °C in the dark. The electrodes in the solutions were then transferred into a 50 mM phosphate buffer (pH 7.5) containing 10 mM KBr and 10 mM triethanolamine (TEOA). Cyclic voltammograms and differential pulse voltammogram were recorded with an electrochemical analyzer (Bioanalytical Systems, BAS-50) under Ar atmosphere. A saturated calomel electrode (SCE) and a Pt plate were used as the reference and the counter electrodes, respectively.

Measurements of photocurrent and action spectrum

In the photocurrent measurement during potential scan, steady photoirradiation was carried out with a 500 W Xe arc lamp (Ushio, UI-502C) through optical filters (Toshiba, IRA-25S × 2 and UV-D33S × 1). Photocurrent was monitored by the light irradiation during 1 mV s^{-1} potential scan to cathodic direction, while the light was turned on and off repeatedly every 50 s interval. In the action spectral measurement at a constant potential, photoirradiation was carried out by the use of a 500 W Xe arc lamp (Ushio, UI-501C) equipped with a grating monochromator (JASCO, CT-10).

Time-resolved fluorescence spectroscopy

The time-resolved fluorescence spectra were measured with second harmonic generation (SHG) (410 nm) of a Ti:sapphire laser (Spectra-Physics, Tsunami 3950-L2S, full width at half-maximum (fwhm) 1.5 ns) as an excitation source and detected with streakscope (Hamamatsu Photonics, C4334-01).[32] All samples were deaerated by Ar bubbling.

Nanosecond time-resolved absorption spectroscopy

The nanosecond time-resolved absorption spectra were measured with SHG (532 nm) of a Nd:YAG laser (Spectra-Physics, Quanta-Ray GCR-130, fwhm 6 ns) as an excitation source. The transient absorption spectra in the visible and near-IR region from 600–1600 nm were detected with a Ge-APD photodiode (Hamamatsu Photonics, B2834).[30] All the samples were contained in a 1 cm quartz cell and were deaerated by Ar bubbling.

Acknowledgement

This work was supported, in part, by the Grant-in-Aids from the Ministry of Education, Culture, Sports, Science and Technologies, Japan and the Asahi Glass Foundation (both for N. N.) and Sasagawa Scientific Research Grant from the Japan Science Society (for H. M.). We thank Professor S. Shinkai, Professor I. Hamachi and Dr S. Kiyonaka for the technical advice to perform the axial-ligand exchange reaction of **1**·Fe-Mb.

References

1 S. H. Friedman, D. L. DeCamp, R. P. Sijbesma, G. Srdanov, F. 1 Wudl and G. L. Kenyon, *J. Am. Chem. Soc.*, 1993, **115**, 6506.
2 E. Nakamura, H. Tokuyama, S. Yamago., T. Shiraki and Y. Sugiura, *Bull. Chem. Soc. Jpn.*, 1996, **69**, 2143 and references therein.
3 T. Tsuchiya, Y. N. Yamakoshi and N. Miyata, *Biochem. Biophys. Res. Commun.*, 1995, **206**, 885.
4 T. Andersson, K. Nilsson, M. Sundahl, C. Weatman and O. Wennerström, *J. Chem. Soc., Chem. Commun.*, 1992, 604.
5 H. Hungerbühler, D. M. Guldi and K. -D. Asmus, *J. Am. Chem. Soc.*, 1993, **115**, 3386.
6 Y. N. Yamakoshi, T. Yagami, K. Fukuhara, S. Sueyoshi and N. Miyata, *J. Chem. Soc., Chem. Commun.*, 1994, 517.
7 H. Tokuyama, S. Yamago and E. Nakamura, *J. Am. Chem. Soc.*, 1993, **115**, 7918; A. M. Cassell, W. A. Scrivens and J. M. Tour, *Angew. Chem., Int. Ed.*, 1998, **37**, 1538; S. Takenaka, K. Yamashita, M. Takagi, T. Hatta, A. Tanaka and O. Tsuge, *Chem. Lett.*, 1999, 319; N. Nakashima, T. Ishii, M. Shirakusa, T. Nakanishi, H. Murakami and T. Sagara, *Chem. Eur. J.*, 2001, **7**, 1766.
8 A. S. Boutorine, H. Tokuyama, M. Takasugi, H. Isobe, E. Nakamura and C. Hélène, *Angew. Chem., Int. Ed.*, 1994, **33**, 2462; R. Bermstein, F. Prat and C. S. Foote, *J. Am. Chem. Soc.*, 1999, **121**, 464.
9 Y.-P. Son, G. E. Lawson, N. Wang, B. Liu, D. K. Moton and R. Dabestani, *Proc. Electrochem. Soc.*, 1997, 645.
10 A. Kurz, C. M. Halliwell, J. J. Davis, H. A. O. Hill and G. W. Canters, *Chem. Commun.*, 1998, 433.
11 J. R. Winkler and H. B. Gray, *Chem. Rev.*, 1992, **92**, 369; I. Hamachi, S. Tanaka and S. Shinkai, *J. Am. Chem. Soc.*, 1993, **115**, 10458; I. Hamachi, Y. Matsugi, K. Wakigawa and S. Shinkai, *Inorg. Chem.*, 1998, **37**, 1592.
12 H. Murakami, Y. Okusa, S. Kiyonaka, I. Hamachi, S. Shinkai and N. Nakashima, *Chem. Lett.*, 2000, 46.
13 H. Imahori, K. Hagiwara, M. Aoki, T. Akiyama, S. Taniguchi, T. Okada, M. Shirakawa and Y. Sakata, *J. Am. Chem. Soc.*, 1996, **118**, 11771; H Imahori, K. Hagiwara, T. Akiyama, M. Aoki, S. Taniguchi, T. Okada, M. Shirakawa and Y. Sakata, *Chem. Phys. Lett.*, 1996, **263**, 545.
14 M. Tamura, T. Asakura and T. Yonetani, *Biochem. Biophys. Acta*, 1973, **295**, 5008.
15 J. J. Stewart, *QCPE Bull.*, 1989, **9**, 10.
16 F. W. Teale, *Biochem. Biophys. Acta*, 1959, **35**, 543.
17 T. Yonetani, *J. Biol. Chem.*, 1967, **242**, 5008.
18 An attempt to reconstitute dicarboxymethano[60]fullerene with apo-Mb was unsuccessful. This fullerene is expected to be too large to incorporate in the crevice of apo-Mb.
19 The concentration of **1**·Fe-Mb aqueous solution was calculated with the molecular extinction coefficient of the Soret-band determined by pyridine-haemochromogen method: see, K. G. Paul, H. Theorell and A. Akeson, *Acta Chem. Scand.*, 1953, **7**, 1284 . The molecular extinction coefficient of the Soret-band in **1**·Fe-Mb determined was 189 000, which is very close to that of native-Mb (188 000). Thus, the concentration of **1**·Zn-Mb aqueous solution

was calculated with the molecular extinction coefficient of the Soret-band in zinc Mb (256 000): see ref. 17.
20 T. Asakura and T. Yonetani, *J. Biol. Chem.*, 1969, **262**, 6725.
21 F. A. Armstrong, H. A. O. Hill and N. Walton, *J. Acc. Chem. Res.*, 1988, **21**, 407; N. Nakashima, Y. Miyata and M. Tominaga, *Chem. Lett.*, 1996, 731; A.-E. F. Nassar, J. F. Rusling, M. Tominaga, J. Yanagimoto and N. Nakashima, *J. Electroanal. Chem.*, 1996, **416**, 183.
22 J. F. Rusling and A.-E. F. Nassar, *J. Am. Chem. Soc.*, 1993, **115**, 11891.
23 D. Dubois, G. Moninot, W. Kutner, M. T. Johns and K. M. Kadish, *J. Phys. Chem.*, 1992, **96**, 7137; T. Nakanishi, H. Murakami, T. Sagara and N. Nakashima, *J. Phys. Chem. B*, 1999, **103**, 304.
24 N. Nakashima, T. Kuriyama, T. Tokunaga, H. Murakami and T. Sagara, *Chem. Lett.*, 1998, 633; N. Nakashima, Y. Nonaka, T. Nakanishi, T. Sagara and H. Murakami, *J. Phys. Chem. B*, 1998, **102**, 7328; N. Nakashima, T. Tokunaga, Y. Nonaka, T. Nakanishi, H. Murakami and T. Sagara, *Angew. Chem., Int. Ed.*, 1998, **37**, 2671; T. Nakanishi, H. Murakami, T. Sagara and N. Nakashima, *Chem. Lett.*, 2000, 340.
25 Cyclic voltammogram for a cast film of 1/TDAB in a 0.5 M TEAC aqueous solution containing 10 mM TEOA showed three redox couples at −350 and −910 mV for $C_{60}^{\bullet -}$ and C_{60}^{2-}, respectively, and −1060 mV for the porphyrin ring.
26 For example, H. Imahori and Y. Sakata, *Adv. Mater.*, 1997, **9**, 537 and references therein.
27 H. Imahori, S. Ozawa, K. Ushida, M. Takahashi, T. Azuma, A. Akiyama, M. Hasegawa, S. Taniguchi, T. Okada and Y. Sakata, *Bull. Chem. Soc. Jpn.*, 1999, **72**, 485.
28 S. Fukuzumi, H. Imahori, H. Yamada, M. E. El-Khouly, M. Fujitsuka, O. Ito and D. M. Guldi, *J. Am. Chem. Soc.*, 2001, **123**, 2571 and references therein.
29 M. Fujitsuka, O. Ito, H. Imahori, K. Yamada, H. Yamada and Y. Sakata, *Chem. Lett.*, 1999, 721.
30 M. Fujitsuka, O. Ito, T. Yamashiro, Y. Aso and T. Otsubo, *J. Phys. Chem. A*, 2000, **104**, 4876.
31 T. Kunitake, N. Kimizuka, N. Higashi and N. Nakashima, *J. Am. Chem. Soc.*, 1984, **106**, 1978.
32 O. Ito, Y. Sasaki, Y. Yoshikawa and A. Watanabe, *J. Phys. Chem.*, 1995, **99**, 9838.